Center for Turbulence Research
Proceedings of the Summer Program 2006

Modeling quasi-two-dimensional turbulence in MHD duct flows

By S. Smolentsev† AND R. Moreau‡

This study considers quasi-two-dimensional magnetohydrodynamic (MHD) flows in a transverse uniform magnetic field in which turbulent structures appear as columnar-like vortices aligned with the field direction. In such flows, viscous and ohmic losses occur in the boundary layers at the flow-confining walls perpendicular to the magnetic field (Hartmann layers). Two eddy-viscosity based turbulence models capturing these specific flow features, zero- and one-equation, are introduced. The results are in fair agreement with the experimental data obtained earlier in the Magnetohydrodynamic Turbulence (MATUR) experiment by Messadek and Moreau (2002) for free shear-layer MHD flows. We also perform a two-dimensional direct numerical simulation (DNS) of a duct flow to address specific near-wall effects associated with the interaction between the vortices generated in the internal shear layer and the MHD boundary layer at the duct wall parallel to the magnetic field. The DNS shows that under certain conditions, the near-wall flow exhibits negative turbulence production. This may limit the applicability of the eddy-viscosity concept in MHD flows.

1. Introduction

The present study is motivated by the need for developing turbulence models for flows in fusion applications. Turbulence modeling is one of the key elements of Fluid Dynamics and Computational Fluid Dynamics (Wilcox 1994). Numerous turbulence models based on the eddy-viscosity concept, including zero, one- , and two-equation models, are available and widely used in industrial, meteorological, and oceanographical applications (Wilcox 1994, Pope 2000), but to a lesser extent in fusion applications, such as breeding blankets of a fusion power-reactor (Harms *et al.* 2000). In the blanket channels, an electrically conducting lithium-containing fluid flows in a strong plasma-confining magnetic field, experiencing an electromagnetic force (Lorentz force), which appears as a result of the interaction between electric currents induced in the fluid and the applied magnetic field. Such flows are known as magnetohydrodynamic (MHD) flows (see, e.g., Moreau 1990). The underlying physics of modeling MHD turbulence is related to the predominant electromagnetic dissipation mechanism (Joule dissipation), which enforces a strong flow anisotropy until the limit of quasi-two-dimensional (Q2D) turbulence is achieved. In contrast to ordinary fluid flows, modeling turbulence in MHD flows, especially in a strong magnetic field, has not yet been fully considered.

MHD flows in a blanket are characterized by four dimensionless parameters: the magnetic Reynolds number Re_m, Hartmann number Ha, Reynolds number Re, and the wall conductance ratio c_w:

† University of California–Los Angeles
‡ Lab. EPM, ENSHM de Grenoble

$$Re_m = \mu_0 \sigma_l U_0 L, \quad Ha = B_0 L \sqrt{\sigma_l/(\nu\rho)}, \quad Re = U_0 L/\nu, \quad c_w = (t_w \sigma_w)/(L\sigma_l).$$

Here, B_0, L, and U_0 are the applied magnetic field, characteristic cross-sectional dimension, and the mean-flow velocity, while μ_0, t_w, σ_w, ρ, ν, and σ_l are the magnetic permeability, wall thickness, wall electrical conductivity, fluid density, kinematic viscosity, and the fluid electrical conductivity correspondingly. Candidate liquids for use in the blanket range from low conductivity molten salts, such as FLiBe or FLiNaBe ($\sigma_l \sim 10^2$ S/m), to high electrical conductivity liquid metals, such as lithium or lead-lithium alloy ($\sigma_l \sim 10^6$ S/m). The Reynolds number in molten-salt and liquid-metal flows is very high (10^4–10^5), so that instabilities are likely to develop and sustain turbulence. On the contrary, the magnetic Reynolds number in the blanket flows is much smaller than unity, so that the induced magnetic field is negligibly smaller than the applied one. In liquid-metal flows $Ha \sim 10^4$–10^5, while $Ha \sim 10^1$–10^2 in molten-salt flows. This parameter plays an important role in MHD wall-bounded flows, where the thickness of the MHD boundary layer at the walls perpendicular to the magnetic field is proportional to $1/Ha$. In particular, it implies that the key parameter in modeling MHD turbulence is the ratio Re/Ha, which can be interpreted as the Reynolds number built through the thickness of the Hartmann layer (Moresco and Alboussière 2004), or as the ratio between the inertia and Lorentz force. This study is limited to the particular case of insulating walls, i.e., $c_w = 0$.

The status of modeling MHD turbulence is illustrated in the *Ha*–*Re* diagram (Fig. 1), where a straight line given by the equation $Ha/Re = (Ha/Re)_{cr}$ separates two subregions with substantially different properties. The critical value of Ha/Re has been evaluated experimentally for different duct shapes and field orientations (see, e.g., Branover 1978) and recently reexamined by Moresco and Alboussière (2004). In the subregion below the separation line, the Joule dissipation reduces the turbulence intensity in the magnetic field direction, while the flow in the perpendicular plane remains marginally affected. As a result, the turbulent flow demonstrates transitional features from three-dimensional to Q2D turbulence as the magnetic field increases. A number of efforts, including RANS models (Kitamura & Hirata 1978, Ji & Gardner 1997, Widlund *et al.* 1998, Kenjers & Hanjalic 2000, Smolentsev *et al.* 2002), LES models (Shimomura 1991, Knaepen & Moin 2004, Kobayashi 2006), and DNS, (e.g., Lee & Choi 2001, Satake *et al.* 2002), have been performed to address MHD turbulent flows in this parameter subdomain. In terms of fusion applications, these studies are mostly relevant to the molten-salt flows but not to the liquid-metal applications, where the Hartmann number is four orders of magnitude higher.

In the subregion above the separation line, turbulence appears in the very specific Q2D form. The conditions leading to Q2D MHD turbulence have been formulated by Sommeria and Moreau (1982). In Q2D turbulent flows, turbulence structures appear as big (comparable in size with the duct dimension) columnar-like vortices with their axis aligned with the field direction. Three-dimensional features can still be observed in the thin Hartmann layers, where all ohmic and viscous losses occur, while the influence of inertia is negligible. Such eddies do not induce much electric current and thus are weakly affected by a magnetic field, persisting over many eddy turnovers, until being damped via dissipating processes in the Hartmann layers. To our knowledge, until now only one attempt has been made to implement a turbulence model relevant to strong magnetic fields leading to Q2D MHD turbulence by Cuevas *et al.* (1997). It is a zero-equation

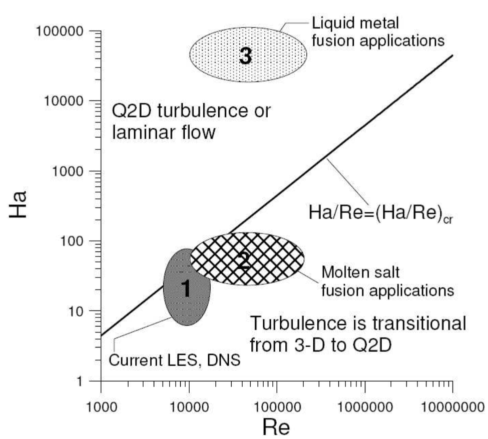

FIGURE 1. *Ha–Re* diagram.

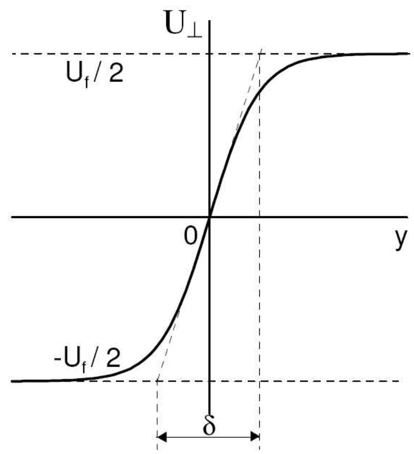

FIGURE 2. Simple shear flow.

model with the eddy viscosity obtained from the renormalization group theory. However, the model was adjusted for a particular liquid-metal flow in the midplane of a rectangular duct with electrically conducting walls and does not specifically address issues of Q2D turbulence.

The present study focuses on MHD wall-bounded flows when turbulence is essentially Q2D and covers the range of parameters specific to the liquid-metal flows in a blanket. The paper consists of two major parts. In Section 2, two eddy-viscosity based turbulence models, zero- and one-equation, are first introduced and then adjusted using the data from the MATUR experiment (Messadek & Moreau 2002). In Section 3, a DNS of Q2D MHD flows in a duct is performed on the basis of the "SM82" equations (Sommeria & Moreau 1982) and the newly developed turbulence models are discussed in light of the DNS data.

2. Turbulence modeling

2.1. *Mean-flow equation*

We consider flows of a viscous, incompressible, electrically conducting liquid in a rectangular duct across a uniform magnetic field, assuming conditions leading to Q2D turbulence. Such flows demonstrate the Hartmann layers at the walls perpendicular to the magnetic field and the core, where the flow is essentially two-dimensional. The starting point in the development of a turbulence model is the standard set of the MHD flow equations for a Q2D flow of electrically conducting fluid in a strong magnetic field known as "SM82" equations, first formulated by Sommeria and Moreau (1982), and then with some variations by Lavrentev *et al.* (1990), Bühler (1996), and Smolentsev (1997). The equations can be obtained by integrating the original three-dimensional flow equations along the magnetic field lines. The result of the integration is a set of two-dimensional equations for the instantaneous velocity field $u_{\perp i}(x,t)$ (i=1, 2) formulated in terms of the core variables:

$$\frac{\partial u_{\perp i}}{\partial t} + u_{\perp j}\frac{\partial u_{\perp i}}{\partial x_j} = -\frac{1}{\rho}\frac{\partial p_\perp}{\partial x_i} + \nu\frac{\partial^2 u_{\perp i}}{\partial x_j \partial x_j} - \frac{u_{\perp i}}{\tau}, \tag{2.1}$$

$$\frac{\partial u_{\perp i}}{\partial x_i} = 0. \tag{2.2}$$

The subscript "$\perp$" indicates that in the modeled core, the velocity component in the magnetic field direction is negligible and the flow occurs in the plane perpendicular to this direction. For the sake of simplicity, we limit ourselves to the case of electrically insulating walls, so that the so-called Hartmann breaking time τ, which is the damping time due to both ohmic and viscous losses in the Hartmann layers, is given by (Sommeria & Moreau 1982):

$$\tau = Ha^{-1}b^2/\nu. \tag{2.3}$$

Here, the Hartmann length b, which is a half-width of the channel, is used as a length scale. This expression can be easily modified to take into account electrical conductance.

As a next step, all flow variables are decomposed into mean and fluctuating parts by using the Reynolds decomposition: $u_{\perp i} = U_{\perp i} + u'_{\perp i}, p_\perp = P_\perp + p'_\perp$ (capital letters are used for the average field, while the "prime" symbol denotes fluctuations), and then Eqs. (2.1) and (2.2) are averaged in the ensemble average sense. In ordinary hydrodynamics, the averaged equations are known as the Reynolds-Averaged Navier-Stokes (RANS) equations. We use the same term in the reference MHD case, where the averaged equations have been obtained in the following form:

$$\frac{\partial U_{\perp i}}{\partial t} + U_{\perp j}\frac{\partial U_{\perp i}}{\partial x_j} = -\frac{1}{\rho}\frac{\partial P_\perp}{\partial x_i} + \frac{\partial}{\partial x_j}\left(\nu\frac{\partial U_{\perp i}}{\partial x_j} - \langle u'_{\perp i}u'_{\perp j}\rangle\right) - \frac{U_{\perp i}}{\tau}, \tag{2.4}$$

$$\frac{\partial U_{\perp i}}{\partial x_i} = 0. \tag{2.5}$$

The only, but important difference with the corresponding non-MHD RANS equations is the additional linear-drag term $U_{\perp i}/\tau$ on the RHS of Eq. (2.4), which models the damping of turbulent vortices at the Hartmann walls. The Reynolds stress $-\rho\left\langle u'_{\perp i}u'_{\perp j}\right\rangle$ still appears on the RHS of Eq. (2.4) as an additional unknown, which needs to be modeled. As in ordinary flows, we apply the Boussinesq approximation, where a turbulent (eddy) viscosity, ν_t, is introduced, such that the turbulent shear stress in a boundary-layer type flow can be described as a product of ν_t and the cross-stream mean velocity gradient:

$$\langle u'v'\rangle = -\nu_t\frac{\partial U}{\partial y}. \tag{2.6}$$

Using relation (2.6), Eq. (2.4) can be rewritten in the following form:

$$\frac{\partial U_{\perp i}}{\partial t} + U_{\perp j}\frac{\partial U_{\perp i}}{\partial x_j} = -\frac{1}{\rho}\frac{\partial P_\perp}{\partial x_i} + \frac{\partial}{\partial x_j}\left((\nu + \nu_{t\perp})\frac{\partial U_{\perp i}}{\partial x_j}\right) - \frac{U_{\perp i}}{\tau}. \tag{2.7}$$

The essence of RANS-based turbulence modeling is obtaining closure relations for the eddy viscosity. Special approaches leading to reasonably simple closures in the case of Q2D MHD turbulence are developed in the subsequent sections.

2.2. *Zero-equation model*

Q2D turbulence usually arises from the instability of an internal parallel shear layer (see, e.g., Tsinober 1975). Therefore, to develop a closure relation for $\nu_{t\perp}$, first consider an elementary problem for a simple shear layer (Fig. 2). The velocity changes occur in the y direction, while a magnetic field is applied in the z direction (perpendicular to the figure plane). Two solid walls, which bound the flow in the z direction, are $2b$ apart. The shear layer has the thickness δ and owes its existence to the *a priori* given forcing velocity U_f. In a strong magnetic field, the flow consists of a core and two Hartmann layers at the walls $z = \pm b$. The core velocity is governed by the following equation:

$$\nu_{t\perp}\frac{d^2U_\perp}{dy^2} - \frac{U_\perp}{\tau} = -\frac{U_f}{2\tau}, \tag{2.8}$$

which is a particular case of Eq. (2.7). An elementary solution of Eq. (2.8) is

$$U_{\perp+} = \frac{U_f}{2}\left[1 - Exp(-y/\sqrt{\nu_{t\perp}\tau})\right]\ y \geq 0;\ U_{\perp-} = -\frac{U_f}{2}\left[1 - Exp(y/\sqrt{\nu_{t\perp}\tau})\right]\ y < 0. \tag{2.9}$$

Based on Eq. (2.9), the thickness of the shear layer is

$$\delta = 2\sqrt{\nu_{t\perp}\tau}. \tag{2.10}$$

Therefore, providing that δ can be evaluated independently, e.g. from experiments, the closure relation for the turbulent viscosity is

$$\nu_{t\perp} = 0.25\delta^2/\tau. \tag{2.11}$$

In accordance with the common terminology used in turbulence modeling, expression (2.11) represents a zero-equation model, since no differential equations are used. The following expression for the thickness of the shear layer entering Eq. (2.11) has been derived by Messadek and Moreau (2002) from their measurements:

$$\frac{\delta}{h} \sim \left(\frac{Ha}{Re}\right)^{-1/2}. \tag{2.12}$$

Here, h is the flow dimension in the direction of the applied magnetic field. It appears that the law given by Eq. (2.11) is rather general provided that the Q2D turbulence conditions can be established.

2.3. *One-equation model*

The obvious shortcomings of the zero-equation model (e.g., $\nu_{t\perp}$ does not vary over the duct cross-sectional area) can be overcome with one-equation models, in which flow history effects can be accounted for. Such models involve a transport equation for the turbulent kinetic energy per unit mass $K_\perp = 0.5\left\langle u'_{\perp i}u'_{\perp j}\right\rangle$.We may express the eddy viscosity as a product of the velocity scale and the characteristic length scale. The natural velocity scale, used in practically all existing eddy-viscosity based models, is the square root of $K_\perp$, while the length scale can be constructed as $\sim \sqrt{K_\perp}\tau$. Finally, the expression for the eddy viscosity takes the following form:

$$\nu_t = C_\nu K_\perp \tau. \tag{2.13}$$

Constant C_ν in Eq. (2.13) needs to be evaluated from experimental data. Similar to the most common formulation of Launder and Spalding (Launder & Spaulding 1974), the desired equation for $K_\perp$ has been obtained here in the following form:

$$\frac{\partial K_\perp}{\partial t} + U_{\perp j}\frac{\partial K_\perp}{\partial x_j} = P_K + \mathit{Diff} - \epsilon_{Ha}. \tag{2.14}$$

The two terms on the left-hand side of Eq. (2.14) are the unsteady term and the convection. The first term on the right-hand side of Eq. (2.14), $P_K = \nu_{t\perp}\left(\frac{\partial U_{\perp i}}{\partial x_j}\right)^2$, is the turbulence production. The second term, $\mathit{Diff} = \frac{\partial}{\partial x_j}\left[\left(\nu + \frac{\nu_{t\perp}}{\sigma_K}\right)\frac{\partial K_\perp}{\partial x_j}\right]$, is the diffusion, which includes the molecular diffusion and its turbulent counterpart. Here, σ_K is the model constant known as the turbulent Prandtl number. The last term, $\epsilon_{Ha} = K_\perp/\tau$, representing ohmic and viscous losses at the Hartmann walls, is specific to Q2D MHD turbulence. The Joule dissipation term does not appear on the RHS of Eq. (2.14), since columnar-like eddy structures, associated with Q2D turbulence, do not induce an electric current. The viscous dissipation term, ϵ, which plays an important role in modeling three-dimensional turbulence, is not included either. Its absence is justified by the fact that in purely two-dimensional turbulence, the direct energy cascade toward smaller scales at the rate ϵ does not exist (Kraichnan 1967). Rather, inverse energy cascade occurs by "vortex cannibalization" events until it is stopped by the dissipation losses in the Hartmann layers or due to geometrical restrictions. Therefore, the turbulent kinetic energy can be calculated directly from Eq. (2.14) providing that σ_K has been specified. Here, we assume $\sigma_K = 1.1$ by analogy with one-equation models used in modeling three-dimensional turbulence (see, e.g., Piquet 1990).

2.4. *Comparison with experimental data*

The models have been tested using experimental data from the MATUR experiment (Messadek & Moreau 2002), where a turbulent azimuthal flow is enforced in the horizontal cylindrical cell of mercury (11 cm radius, 1 cm height) by the action of a steady vertical magnetic field and a radial electric current (Fig. 3a). The location of the shear layer and that of the maximum velocity in the cell are controlled by the internal electrode embedded in the bottom disk at the distance of 5.4 cm from the cell center. The cell is bounded at the top and bottom by non-conducting disks, which are the Hartmann walls. Generation of turbulence occurs in the internal shear layer associated with the inflection point in the "M-type" velocity profile. The flow in the cell is controlled through changes in Re and Ha by varying the electric current and the magnetic field in a wide range, over which turbulence exhibits two-dimensional features.

Figure 3b compares the MATUR experiment data with the velocity profiles computed numerically based on the mean-flow equations formulated in Section 2.1 and using the zero- and one-equation models presented in Sections 2.2 and 2.3. In the calculations, the eddy viscosity was corrected by introducing a wall-damping factor $f(r)$. The function $f(r)$ varies exponentially from zero to one within the boundary layer at the cylindrical wall. Introducing the wall-damping factor is necessary to prevent the models from producing false turbulence near the cylindrical wall, where ordinary three-dimensional turbulence is suppressed by a strong magnetic field. Constant C_ν entering expression (2.13) for the eddy viscosity has been adjusted to give the best fit with the experimental data at $C_\nu = 0.03$. Both models demonstrate a reasonably good agreement with the experimental

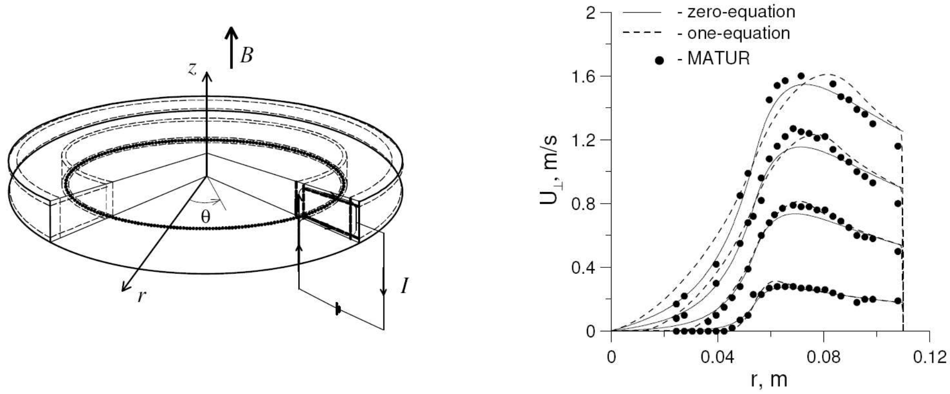

(a) (b)

FIGURE 3. (a) Sketch of the MATUR experiment. (b) Comparison between the MATUR experiment and modeling, using present zero- and one-equation models. $B_0 = 5\,T$; $I = 10;\ 30;\ 50;\ 70A$ (from the lower to the upper curve).

mean-velocity profiles. However, the one-equation model offers a few advantages over the zero-equation model, resulting in more realistic coordinate-dependent distributions of the eddy viscosity.

3. Two-dimensional DNS of turbulent MHD flow in a duct

3.1. *Problem formulation*

In addition to the previously mentioned MATUR experiment, many other experiments were performed under various flow conditions that eventually led to Q2D turbulence (Kolesnikov 1972 and 1985, Reed & Picologlou 1989, Burr *et al.* 2000, Andreev *et al.* 2006). Bühler (1996) performed the first numerical simulations for such a flow for a duct with an electrically conducting strip embedded in the duct wall. Flow instabilities leading to turbulent-like flow patterns were also observed in numerical computations for duct flows in a fringing magnetic field (Morley *et al.* 2004). In spite of their apparent great diversity, in all the examples given above, the Q2D MHD flows share a common property. Namely, turbulence is generated in the internal shear layer associated with the inflection point. It is therefore reasonable to focus on this common flow feature, rather than examining details of a particular MHD duct flow. For this purpose, we consider a "generalized" MHD flow in a rectangular duct submitted to a uniform transverse magnetic field. The duct cross-sectional dimensions are $2b$ (in the field direction) and $2a$. The flow is driven by a pressure gradient and is opposed by a volumetric force, which is responsible for forming the M-type velocity profile. Figure 4 shows schematically the midplane of the flow. The volumetric force is applied over the whole channel length l. Its distribution is sketched in Fig. 4, and is given through the following expression, which parameterizes the Lorentz force term:

$$F(y) = \frac{F_0}{1 + [\sinh(\frac{y-d}{L})/\sinh(\frac{y_0}{L})]^m}. \qquad (3.1)$$

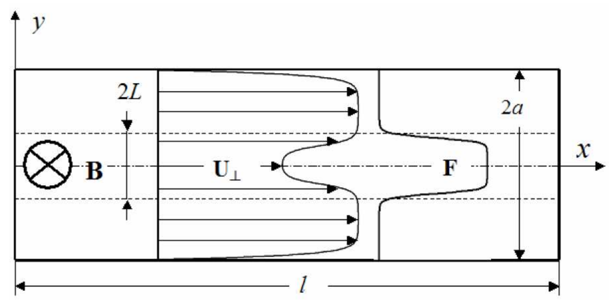

FIGURE 4. Mid-plane of the Q2D turbulent MHD flow in a rectangular duct.

In the calculations presented below, $m = 10$, $d = 0$, and $y_0/L = 1$.

This reference MHD flow problem is governed by the SM82 equations for the core variables, which are written here in a dimensionless form:

$$\frac{\partial U}{\partial t} + U\frac{\partial U}{\partial x} + V\frac{\partial U}{\partial y} = -\frac{\partial P}{\partial x} + \frac{1}{Re}\left(\frac{\partial^2 U}{\partial x^2} + \frac{\partial^2 U}{\partial y^2}\right) - \frac{Ha}{Re}\left(\frac{L}{b}\right)^2 U - \frac{1}{Fr_*}\frac{F}{F_0},$$

$$\frac{\partial V}{\partial t} + U\frac{\partial V}{\partial x} + V\frac{\partial V}{\partial y} = -\frac{\partial P}{\partial y} + \frac{1}{Re}\left(\frac{\partial^2 V}{\partial x^2} + \frac{\partial^2 V}{\partial y^2}\right) - \frac{Ha}{Re}\left(\frac{L}{b}\right)^2 V, \qquad (3.2)$$

$$\frac{\partial U}{\partial x} + \frac{\partial V}{\partial y} = 0.$$

The half-width L was used as the length scale so that the Reynolds number and the modified Froude number ($Fr_* = U_0^2/F_0 L$) are both built through L, while the Hartmann number is built through the Hartmann length b. Equations (3.2) have been rewritten in the equivalent form in terms of the vorticity and the stream function, and then solved numerically with a well-established ψ–ω approach (see, e.g., Tannehill *et al.* 1997) using periodic boundary conditions at the flow inlet and outlet on a uniform mesh with 512 and 401 points in the x- and y-direction, correspondingly. For particular combinations of the flow parameters, the flow becomes unstable and eventually turbulent.

3.2. *Results and discussion*

The purpose of this DNS was to address the issues of interaction between the "active" internal shear layer and the "passive" boundary layer at the duct wall parallel to the magnetic field. When such flows exhibit wall jets and M-shape mean-velocity profiles, the turbulent shear-layer thickness depends on both Ha and Re. The distance between the shear layer and the parallel wall is in turn dictated by the Hartmann number. Then, generally speaking, the internal shear layer cannot be treated as a purely free shear layer, especially at high Ha and Re. The near-wall interactions are particularly important from the point of view of heat transfer when an external heat flux is applied to the wall. If strong enough, these interactions may also significantly limit the applicability of the turbulence models developed in the present study, where the internal shear layer was considered without being affected by the parallel wall. Note that the turbulent pulsations near the parallel wall were measured by Burr *et al.* (2000), who observed that, depending on Ha and Re, the vortices in the near-wall region can rotate either clockwise or counterclockwise and the instability is correspondingly associated with the inner or

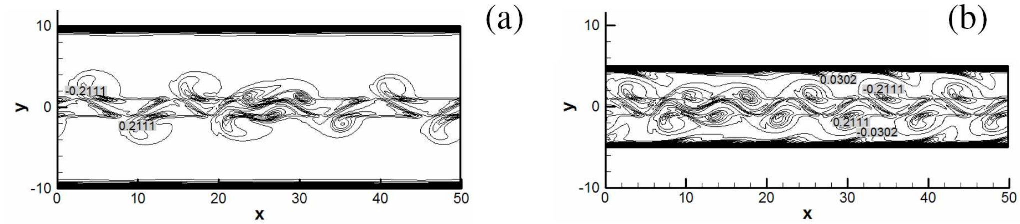

FIGURE 5. Vorticity distribution in the reference flow: (a) wide duct, $L/a = 0.1$; and (b) narrow duct, $L/a = 0.2$. $Ha = 500$, $Re = 1000$, $Fr_* = 125$, $l/L = 50$, and $b/L = 0.2$.

outer side of the high-velocity near-wall jet. These two regimes were referred to as Type I and Type II instabilities.

In the present DNS, the location of the shear layer with respect to the parallel wall can be changed easily by varying the parameters entering expression (3.1). Two cases have been computed (Fig. 5) and their results compared to reveal the wall effect. In the case of a "wide" duct, the parameter L/a was set at 0.1. In the case of a "narrow" duct, $L/a = 0.2$. The other parameters are the same in both cases: $Ha = 500$, $Re = 1000$, $Fr_* = 125$, $l/L = 50$, and $b/L = 0.2$. In both cases, instabilities develop in the internal shear layers, resulting in a double row of counter-rotating vortices whose characteristic size is comparable with the dimension $2L$. The vortices are regularly distributed in space. However, significant irregularities in the flow can be observed in the form of "compound vortex islands," where a few vortices group together to form a bigger structure. This is a clear evidence of the Q2D turbulent flow dynamics. In the wide duct flow, the vortices remain localized within the internal layer without interacting with the parallel boundary layer at the duct walls. However, as expected, in the narrow duct flow, such an interaction occurs. The result of this interaction is seen in Fig. 5b in the form of secondary vortices, which appear when a fast rotating primary vortex moves along the near-wall boundary layer. The observed phenomenon resembles Type I and II instabilities in the Burr *et al.* (2000) experiments, where the vorticity sign near the parallel wall depends on Ha and Re, and thus these experimental observations can be attributed to the interactions between the near-wall liquid and the eddies formed on the internal side of the near-wall jet.

More interpretations of this phenomenon are based on the statistically averaged data shown in Fig. 6. The main differences between the narrow and wide duct flows can be seen in the near-wall region. The wall effect on the shear-layer flow is not present in the wide duct flow but is significant in the narrow duct flow. The most pronounced feature here is the negative turbulence production in the narrow duct near the walls. Negative turbulence production means that the eddy viscosity (not shown here), defined in a formal way as the ratio between the Reynolds stress and the mean velocity gradient, is also negative. It should be mentioned that negative eddy viscosity near the parallel wall can also be noticed in the Burr *et al.* (2000) experiments (not recognized in the original paper by the authors themselves). This is additional evidence of the fact that in any MHD duct flow with the M-shape velocity profile, the distinctive feature is the interaction of the primary vortices with the boundary layer at the parallel wall. Negative eddy viscosity has also been observed in many other flows and is typical of two-dimensional turbulence (Tsinober 2001). This raises the following question: Is the presence of some negative turbulence production a limitation on the applicability of the turbulence models developed? Note,

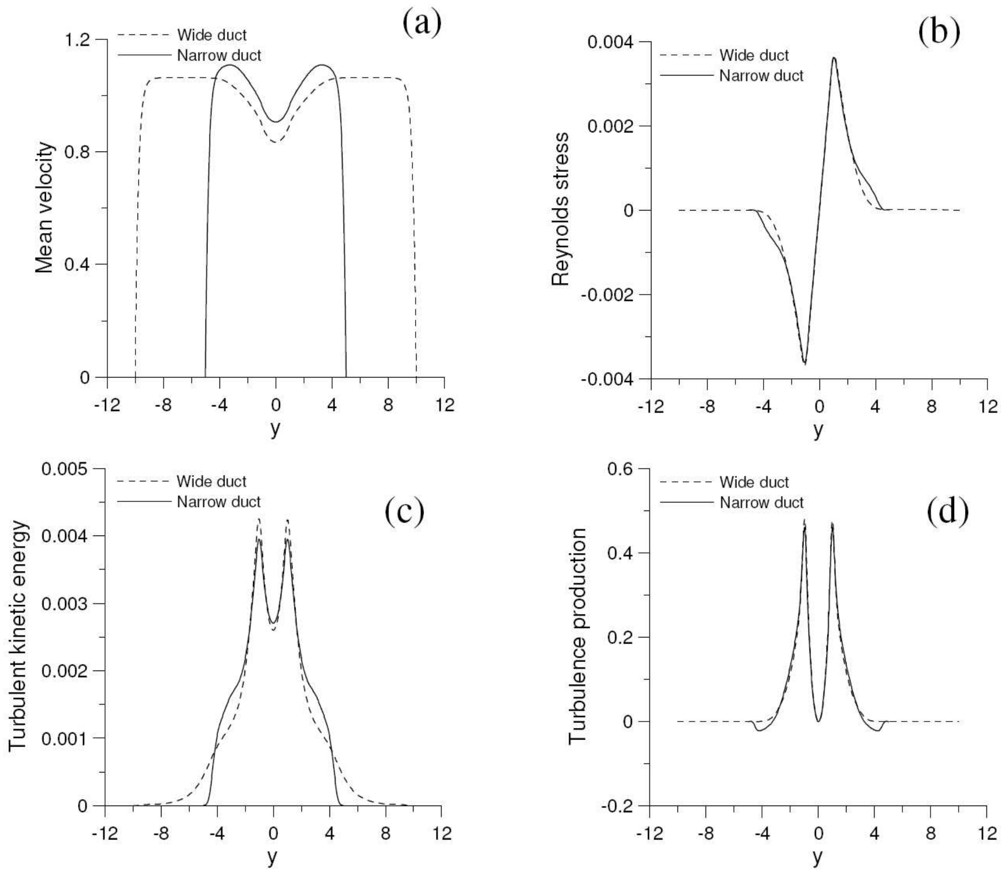

FIGURE 6. Turbulence statistics in the reference flow: (a) mean velocity profile, (b) Reynolds stress, (c) turbulent kinetic energy, and (d) turbulence production.

however, that this limitation is not relevant to the purely free shear-layer flows, e.g. MATUR, where the wall effect is not important.

4. Conclusions

We have developed two eddy-viscosity based models for MHD wall-bounded MHD flows in a strong magnetic field when turbulence becomes Q2D. The models differ from those used in modeling ordinary turbulent flows or in modeling MHD flows where turbulence is transitional from three- to two-dimensional. The differences are related to the specific features of Q2D turbulence, such as the absence of the viscous and Joule dissipation in the core and the localization of both viscous and ohmic losses within the Hartmann layers. The absence of the viscous dissipation in the core associated with the inverse energy cascade explains why using zero- or one-equation models is more reasonable than using the more popular two-equation models. To our knowledge, the present models are the first ones resulting in good agreement with the experimental data for the Q2D MHD flows obtained earlier in the MATUR experiment. All previous RANS models (such those mentioned in Section 1) completely suppress turbulence in strong magnetic field conditions. The one-equation model has some advantages over the zero-equation model since it incorporates the flow history effects via the transport equation for the turbulent kinetic energy. The models, however, exhibit the same limitations typical to this class of turbulence models for ordinary flows. Moreover, as the present DNS shows, the models are not fully adequate in the case of flows where the effects due to the parallel wall are important. The parallel wall effects, as found, are associated with the interaction of the primary vortices generated in the internal shear layer with the flow in the adjacent MHD boundary layer. This interaction results in negative turbulence production and negative eddy viscosity near the corresponding wall, an effect that cannot be described in terms of the eddy-viscosity concept.

Acknowledgments

This study was performed during the 2006 Summer Program at the Center for Turbulence Research with financial support from Stanford University and NASA Ames Research Center. The authors would like to thank Parviz Moin and all CTR staff members for hospitality. The authors are also grateful to Andre Thess, Oleg Zikanov, Stavros Kassinos and Karim Messadek for technical discussions and valuable comments. The support from Mohamed Abdou and his advice regarding fusion applications is greatly appreciated.

REFERENCES

Andreev, O., Kolesnikov, Yu., Thess, A. 2006 Experimental study of liquid metal channel flow under the influence of a nonuniform magnetic field. *Phys. Fluids*, **18**, 065108.

Branover, H. 1978 Magnetohydrodynamic Flows in Ducts. Halsted Press.

Bühler, L. 1996 Instabilities in quasi-two-dimensional magnetohydrodynamic flows. *J. Fluid Mech.* **326**, 125–150.

Burr, U., Barleon, L., Müller, U., Tsinober, A. 2000 Turbulent transport of momentum and heat in magnetohydrodynamic rectangular duct flow with strong sidewall jets. *J. Fluid Mech.* **406**, 247–279.

Cuevas, S., Picologlou, B. F., Walker, J. S., Talmage, G. 1997 Liquid metal MHD flow in rectangular ducts with thin conducting or insulating walls: laminar and turbulent solutions. *Int. J. Eng. Sci.*, **35**, 485–503.

Harms, A. A., Schoepf, K. F., Miley, G. H., Kingdon, D. R. 2000 Principles of Fusion Energy. World Scientific.

Ji, H.-C., Gardner, R. A. 1997 Numerical analysis of turbulent pipe flow in a transverse magnetic field. *Int. J. Heat Mass Trans.*, **40**, 1839–1851.

Kenjeres, S., Hanjalic, K. 2000 On the implementation of effects of Lorentz force in turbulence closure models. *Int. J. Heat Fluid Flow*, **21**, 329–337.

Kitamura, K., Hirata, M. 1978 Turbulent heat and momentum transfer for electrically conducting fluid flowing in two-dimensional channel under transverse magnetic field. *Proc. 6th Int. Heat Transfer Conf.*, Toronto, Canada, **3**, 159.

Knaepen, B. & Moin, P. 2004 Large-eddy simulation of conductive flows at low magnetic Reynolds number. *Phys. Fluids*, **16**, 1255–1261.

Kobayashi, H. 2006 Large eddy simulation of magnetohydrodynamic turbulent channel flows with local subgrid-scale model based on coherent structures. *Phys. Fluids*, **18**, 045107.

Launder, B. E., Spaulding, D. B. 1974 The numerical computation of turbulent flows. *Computer Methods in Appl. Mech. Eng.*, **3**, 269-289.

Kolesnikov, Yu. B. 1972 Two-dimensional turbulent flow in a channel with inhomogeneous electrical conductivity of the walls. *Magnetohydrodynamics*, **8**, 308–312.

Kolesnikov, Yu. B. 1985 Experimental investigation of instability of plane-parallel shear flow in a magnetic field. *Magnetohydrodynamics*, **21**, 47–53.

Kraichnan, R. H. 1967 Inertial ranges in two-dimensional turbulence. *Phys. Fluids* **10**, 1417–1423.

Lavrentiev, I. V., Molokov, S. Yu., Sidorenkov, S. I., Shishko, A. R. 1990 Stokes flow in a rectangular magnetohydrodynamic channel with nonconducting walls within a nonuniform magnetic field at large Hartmann numbers. *Magnetohydrodynamics*, **26**, 325–338.

Lee, D., Choi, H. 2001 Magnetohydrodynamic turbulent flow in a channel at low magnetic Reynolds number. *J. Fluid Mech.*, **439**, 367–394.

Messadek, K. & Moreau, R. 2002 An experimental investigation of MHD quasi-two-dimensional turbulent shear flows. *J. Fluid Mech.*, **456**, 137–159.

Moreau, R. 1990 Magnetohydrodynamics. Kluwer.

Moresco, P. & Alboussière, T. 2004 Experimental study of the instability of the Hartmann layer. *J. Fluid. Mech.*, **504**, 167–181.

Morley, N. B., Smolentsev, S., Munipalli, R., Ni, M.-J, Gao, D., Abdou, M. 2004 Progress on the modeling of liquid metal, free surface, MHD flows for fusion liquid walls. *Fus. Eng. Design*, **72**, 3–34.

Piquet, J. 1990 Turbulent Flows, Models and Physics. Springer.

Pope, S. B. 2000 Turbulent Flows. Cabridge University Press.

Reed, C. B., Picologlou, B. F. 1989 Sidewall flow instabilities in liquid metal MHD flow under blanket relevant conditions. *Fusion Technol.*, **15**, 705–715.

Satake, S., Kunugi, T., Smolentsev, S. 2002 DNS of turbulent pipe flow in a transverse magnetic field. *J. Turbulence*, **3**, 020.

Shimomura, Yu. 1991 Large eddy simulation of magnetohydrodynamic turbulent channel flows under uniform magnetic field. *Phys. Fluids A*, **3**, 3098–3106.

Smolentsev, S. 1997 Averaged model in MHD duct flow calculations. *Magnetohydrodynamics*, **33**, 42–47.

Smolentsev, S., Abdou, M., Morley, N., Ying, A., Kunugi, T. 2002 Application of the "K-ϵ" model to open channel flows in a magnetic field. *Int. J. Eng. Sci.*, **40**, 693–711.

Sommeria, J. & Moreau, R. 1982 Why, how, and when, MHD turbulence becomes two-dimensional. *J. Fluid. Mech.*, **118**, 507–518.

Tannehill, J. C., Anderson, D. A., Pletcher, R. H. 1997 Computational Fluid Mechanics and Heat Transfer. Taylor & Francis.

Tsinober, A.B. 1975 Magnetohydrodynamic turbulence. *Magnetohydrodynamics*, **11**, 7–22.

Tsinober, A. 2001 An informal Introduction to Turbulence. Kluwer.

Widlund, O., Zahrai, S., Bark, F. H. 1998 Development of a Reynolds stress closure for modeling of homogeneous MHD turbulence. *Phys. Fluids*, **10**, 1987–1996.

Wilcox, D. C. 1994 Turbulence Modeling for CFD. DCW Industries, Inc.